

Article

Experiment and Molecular Dynamic Simulation on Performance of 3,4-Bis(3-nitrofurazan-4-yl)furoxan (DNTF) Crystals Coated with Energetic Binder GAP

Yue Qin ¹, Junming Yuan ^{1,*}, Hu Sun ¹, Yan Liu ¹, Hanpeng Zhou ¹, Ruiqiang Wu ², Jinfang Chen ² and Xiaoxiao Li ²¹ School of Environmental and Safety Engineering, North University of China, Taiyuan 030051, China² Shanxi North Xing'an Chemical Industry Co., Ltd., Taiyuan 030008, China

* Correspondence: junmyuan@163.com

Abstract: To investigate the crystallization of DNTF in modified double-base propellants, glycidyl azide polymer (GAP) was used as the coating material for the in situ coating of DNTF, and the performance of the coating was investigated to inhibit the crystallization. The results show that GAP can form a white gel on the surface of DNTF crystals and has a good coating effect which can significantly reduce the impact sensitivity and friction sensitivity of DNTF. Molecular dynamics was used to construct a bilayer interface model of GAP and DNTF with different growth crystal surfaces, and Molecular dynamics calculations of the binding energy and mechanical properties of the composite system were carried out. The results showed that GAP could effectively improve the mechanical properties of DNTF. The values of K/G , γ and ν are higher than those of DNTF crystals, and the values of C_{12} - C_{44} are positive, indicating that GAP can improve DNTF ductility while also improving toughness. Combining the experimental results with the simulation calculations, energetic binder GAP can be referred to as a better cladding layer for DNTF, which is feasible for inhibiting the DNTF crystallization problem in propellants.



Citation: Qin, Y.; Yuan, J.; Sun, H.; Liu, Y.; Zhou, H.; Wu, R.; Chen, J.; Li, X. Experiment and Molecular Dynamic Simulation on Performance of 3,4-Bis(3-nitrofurazan-4-yl)furoxan (DNTF) Crystals Coated with Energetic Binder GAP. *Crystals* **2023**, *13*, 327. <https://doi.org/10.3390/cryst13020327>

Academic Editors: Thomas M. Klapötke, Rui Liu, Yushi Wen and Weiqiang Pang

Received: 30 January 2023

Revised: 11 February 2023

Accepted: 13 February 2023

Published: 15 February 2023



Copyright: © 2023 by the authors. Licensee MDPI, Basel, Switzerland. This article is an open access article distributed under the terms and conditions of the Creative Commons Attribution (CC BY) license (<https://creativecommons.org/licenses/by/4.0/>).

Keywords: 3,4-Bis(3-nitrofurazan-4-yl) furoxan (DNTF); crystallization; energetic binder GAP; mechanical sensitivity; molecular dynamics simulation

1. Introduction

In view of the low danger of DNTF synthesis, the simple preparation process, the high energy, high density, low melting point, and other high qualities, its comprehensive performance due to HMX is close to that of CL-20, making it a better application in the field of modified double-base propellants [1–3]. However, as more research on DNTF's application in propellants is conducted, its flaws are gradually revealed. Pang Jun et al. [4] found that the tablets prepared from DNTF-CMDB propellant by a high-temperature calendaring process have a crystallization phenomenon in the process of natural cooling and storage, which not only affects the appearance but also causes adverse effects such as increased propellant sensitivity, ignition difficulties, and changes in ballistic performance. The crystallization phenomenon was first found in RDX-containing propellants [5–7], and research shows that the propellant preparation process, the species and content of added energy-containing materials, and their solubility in the double-base solid solvent will have an impact on the crystallization, as will the surface coating method, the addition of low surface energy substances, and other means to inhibit crystallization and get a better effect. The crystallization phenomenon will also occur in the propellant containing DNTF, which will occur due to the content of DNTF and the solvent in the formula. Zheng Wei et al. [8] conducted a study on the inhibition of crystallization in modified dual-base propellants containing DNTF, and the amount of crystallization can be significantly reduced by using acetone solution coated with 3% NC, or adding a small amount of polymer to the propellant formulation can completely inhibit crystallization, but there is no study on the binder as

a coating layer of DNTF explosive crystals as a means of inhibition. There is very little existing literature on the mechanism and inhibition of DNTF crystallization in modified double-base propellants at home and abroad. In this paper, we try to use an energetic binder to cover DNTF to form microsphere particles to achieve the effect of propellant crystallization inhibition.

It is critical to fully consider the properties of both the material and the composite system when selecting the cladding material to ensure that the propellant energy, ignition, density, and other characteristics are maintained while effectively improving the crystallization of DNTF and maintaining stable control of its crystallization amount. The azide binder is one of the more prominent types of energetic binder in the field of solid propellants because of its advantages in heat generation, high density, and low mechanical sensitivity [9,10]. In addition, the surface energy of GAP can be compared with that of adhesive. In addition, GAP has the advantage of surface energy and adhesion, which can be used as a DNTF cladding layer to try to investigate the crystallization inhibition method.

The energetic binder glycidyl azide polymer (GAP) was used as the coating material in this paper, and the in situ polymerization method was used to coat and granulate DNTF explosive particles. The morphological properties and mechanical sensitivity changes of the coated samples were studied, and the binding energy and mechanical properties of the composite system model of GAP and DNTF were calculated and analyzed using molecular dynamics simulations. Combining the experimental data and simulation results, we analyze the coating effect of energetic binder GAP on DNTF explosive particles and provide some experimental and theoretical support for improving the crystallization of DNTF in propellant.

2. Materials and Methods

2.1. Experiments and Apparatus

Materials: DNTF, purity > 99%, provided by the Xi'an Institute of Modern Chemistry, Xi'an, China; GAP, Li Ming Chemical Research Institute, Luoyang, China; curing agent (IPDI), BASF SE, Ludwigshafen Germany; tetrahydrofuran, Sinopharm Chemical Reagent Co., Ltd., Shanghai, China.

Instruments: PTY-A type analytical balance, Guangzhou Shangbo Electronic Technology Co., Ltd., Guangzhou, China; HH-SI single-hole thermostatic water bath, Gongyi Yuhua Instrument Co., Ltd., Gongyi, China; BGX-70L electric thermostatic blast drying oven, Suzhou Taiyou Mechanical Manufacturing Co., Ltd., Suzhou, China; SEM-30PLUS scanning electron microscope, Beijing Tianyao Technology Co., Ltd. (coxem China), Beijing, China.

2.2. GAP-Coated DNTF Experiment

The prepared DNTF, binder, curing agent, and solvent, tetrahydrofuran, were placed in a conical flask and mixed at 300 rpm/min for 1 hour at room temperature with ventilation turned on and the outer protective glass of the bench closed during the experiment. After the completion of the coating experiment, the specimens were poured into the surface dish and dried naturally to obtain the product.

2.3. Performance Characterization

SEM: The particle morphology of the coated microsphere samples was observed by scanning electron microscopy (SEM) and compared with that of the DNTF raw material. The samples were all treated with gold spraying and accelerated to 15 KV.

Mechanical sensitivity: Referring to GJ772A-97 Methods 601.1 and 602.1, the WL-1 impact sensitivity meter and the WM-1 friction sensitivity meter were used to test the impact sensitivity and friction sensitivity of DNTF and GAP-coated DNTF samples, respectively: For the impact sensitivity test (25 cm drop height, 30 mg dosage), a 2 kg drop hammer was used; for the friction sensitivity test (pressure 2.45 MPa, swing angle 66°, 20 mg).

2.4. Molecular Dynamics Simulation

With reference to the literature [11–13], the molecular structure of the composite system was modeled using the Visualizer module in Materials Studio software, and after geometric optimization, MD simulations were performed under the NVT ensemble synthesis in the Compass force field.

2.4.1. Vacuum Morphology Prediction of DNTF Crystals

The crystal structure data of DNTF was obtained based on the Cambridge Organic Crystal Database (CCDC) and imported into the Materials Studio simulation platform. The Forcite module was used to optimize molecular configuration and energy. The following optimization parameters were set: compass force field, “medium” accuracy, and “smart” method to optimize the cell parameters. The Bravais-Friedel-Donnary-Harker (BFDH) and Attachment Energy method (AE) in the Morphology Tools module were used to predict the vacuum morphology of DNTF crystals and obtain the surface distribution of DNTF crystals grown under vacuum conditions. Theoretically, the crystalline surface with the largest surface occupation area has the most important effect on the adhesive-filler interfacial bonding performance [14,15]. In this simulation, the interfacial interaction between GAP molecules and DNTF crystals was calculated by selecting the crystal surfaces that occupied more surface area. The vacuum growth morphology of DNTF crystals is shown in Figure 1, the left is the vacuum growth morphology of DNTF crystal in BFDH model and the right is the vacuum growth morphology of DNTF crystal in the AE model. In the figure, nitrogen is shown in blue, oxygen in red and carbon in gry. The first two growth surfaces and their corresponding percentages are listed in Table 1.

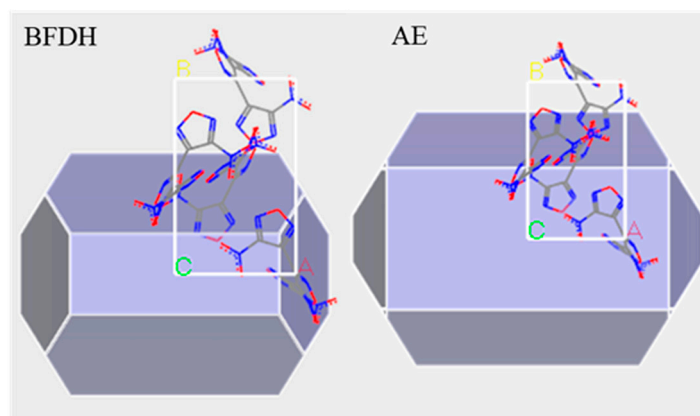


Figure 1. Vacuum growth morphology of DNTF.

Table 1. Natural growth of DNTF crystals crystal surface data.

Crystal	(h k l)	AE/(kcal·mol ⁻¹)	Percentage of Total Area/%
DNTF	(0 1 1)	−48.2498	53.3037
	(1 0 1)	−75.0550	24.3655

2.4.2. Model Construction of Different Crystal Surfaces of the DNTF and Polymer Interface

The modeling of the interaction between different crystal surfaces of the polymer GAP and DNTF is illustrated by the example of the GAP and DNTF (0 1 1) surfaces (see Figure 2). The supercell model of DNTF(0 1 1) surface and the AC box established by polymer GAP construct GAP-DNTF(0 1 1) interfacial crystal model.

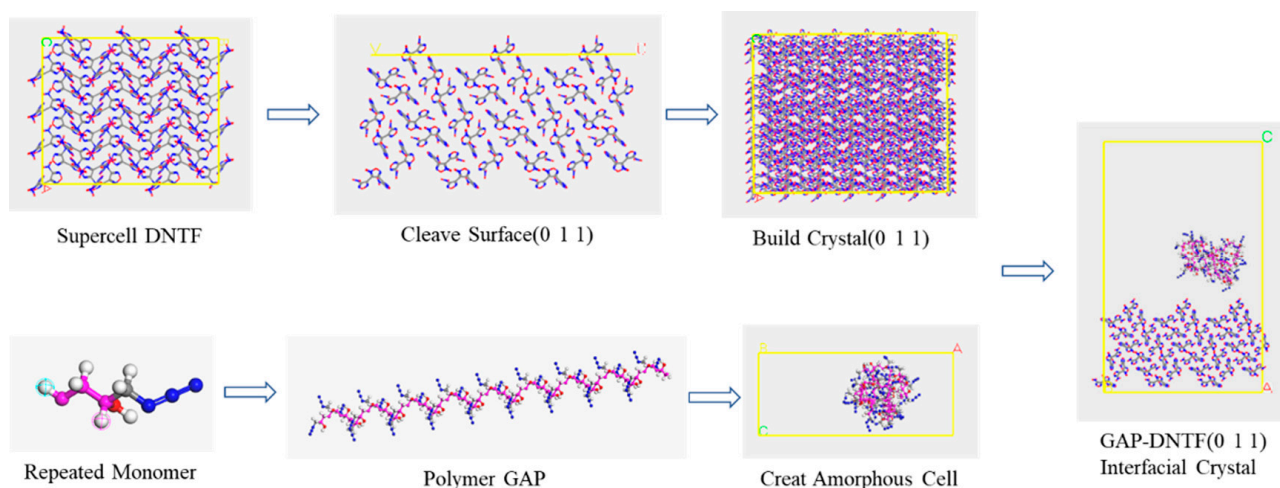


Figure 2. Establishing the interfacial crystal process.

Firstly, a homopolymer ball-and-stick structure model with a degree of polymerization of 35 was developed based on the GAP molecular formula, where the GAP binder polymer contains 35 monomers [14]. Geometry optimization of the Forcite module was selected for molecular mechanics optimization to adjust the structure and conformation of the molecules.

The polymer-bound explosive model was constructed as follows: Firstly, the $4 \times 3 \times 3$ supercell structure of DNTF was built and cut along the main growth plane (0 1 1); the vacuum-free crystal structure of DNTF (0 1 1) crystal plane was constructed; the amorphous structure of GAP molecular chain (Amorphous Cell) was constructed according to its lattice size; and their bilayer interface crystal models were obtained by the Build Layers function, where the vacuum layer Repeat the above method to obtain the bilayer interface model of GAP and other crystal surfaces of DNTF. The model construction needs to be combined with the mass ratio of energetic binder GAP to DNTF in the actual experiment, so only one GAP molecular chain is selected here for AC box construction. In addition, all steps in the model construction process need to be optimized for structure so that the system exhibits the minimum energy at each step, which is because the system loses its initial structure at each step of operation and the energy will be higher than its most stable structure.

2.4.3. Molecular Dynamics Calculation Setup

First, the geometry of the constructed interface model is optimized, and the optimization parameters are set as described in the previous section. Based on the optimized interface model, MD simulations under an isothermal isobaric (NVT) system were performed. The simulation parameters are set as follows: The temperature control method is Anderson, the time step is 1.0 fs, and the total simulation time is 200 ps, in which the first 100 ps steps are used for thermodynamic equilibrium and the last 100 ps steps are used for statistical analysis. During the simulation, van der Waals forces and electrostatic interactions are calculated using atom-based and Ewald methods, respectively, and the results are output once every 1000 steps for a total of 50 frames. The system reaches kinetic equilibrium when the fluctuation range of temperature and energy is less than 5%, and the obtained equilibrium structure is analyzed to obtain the binding energy and mechanical property parameters between components.

3. Results and Discussion

This section may be divided by subheadings. It should provide a concise and precise description of the experimental results, their interpretation, as well as the experimental conclusions that can be drawn.

3.1. Microscopic Morphological Characterization of Particles

SEM was used to characterize the microscopic morphology of DNTF explosive particles and energetic binder GAP-coated DNTF particles. In Figure 3, electron microscopic images of grain morphology characteristics of DNTF explosive are shown in a, b and c which are images of DNTF grain enlarged 50, 500 and 1000 times, respectively. The surface of DNTF without coating treatment is smooth and flat, and the grains are in the shape of regular polyhedra, with a few smaller grains attached to the surface of the grains and no other attachments. It is compatible with the crystalline shape under vacuum and can be used as a benchmark reference for the comparison of GAP binder-coated DNTF samples.

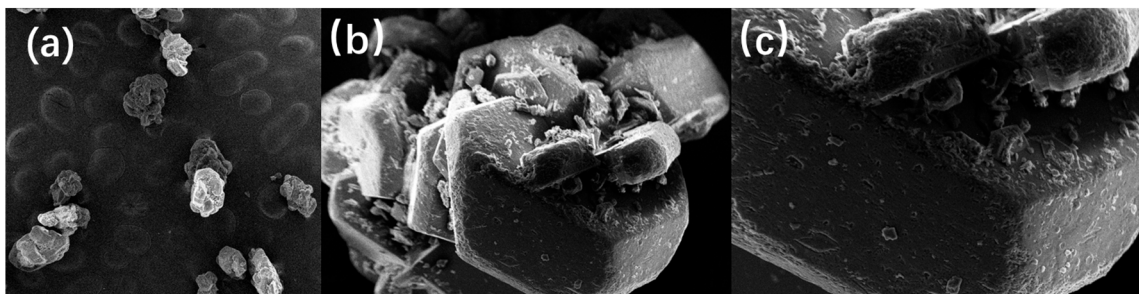


Figure 3. Electron microscopy of DNTF grain morphology: (a) 50 times; (b) 500 times; (c) 1000 times.

In Figure 4, subfigures a, b and c are the electron microscopic morphology of the coated grains at magnifications of 500, 1000, and 5000, respectively. It can be observed that the roughness of the DNTF surface increases after GAP coating, and GAP adheres more small particles of DNTF to the surface of large particles. After magnification, it can be observed that the surface of the original DNTF grains is in a white gel state, and the surface of the grains is basically covered by a thin layer of GAP completely and uniformly. It is consistent with the growth of different crystal surfaces under MS vacuum, which indicates that the GAP-coated DNTF crystals have a good coating effect.

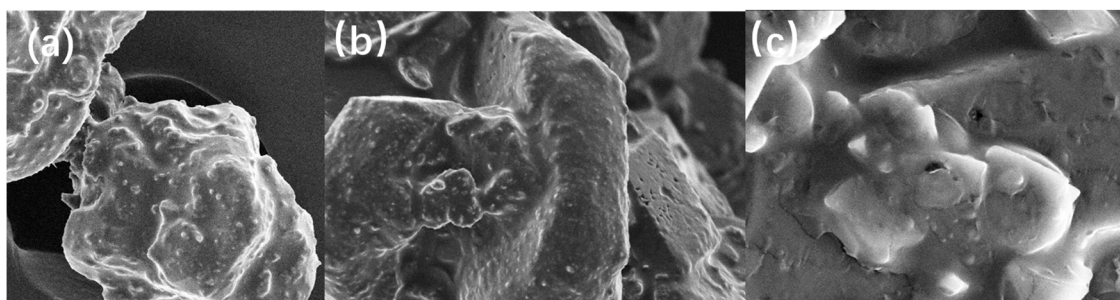


Figure 4. Electron microscopic morphology of coated grains: (a) 500 times; (b) 1000 times; (c) 5000 times.

3.2. Mechanical Sensitivity Analysis

The results of impact and friction sensitivity tests for DNTF and GAP/DNTF cladding are shown in Table 2. Test data of mechanical sensitivity of energetic binder GAP was obtained from the literature [15]. As can be seen from the table, the DNTF explosive grains themselves have high sensitivities, with impact and friction sensitivities of 76% and 100%, respectively; the impact and friction sensitivities of the DNTF grains after GAP cladding are reduced to 48% and 52%, respectively, indicating that the energetic binder GAP as a cladding layer for DNTF crystals can significantly reduce the mechanical sensitivities of DNTF, which will help to improve the safety of DNTF explosives.

Table 2. Impact and friction sensitivity test results.

Sample	Impact Sensitivity/%	Friction Sensitivity/%
GAP	0	0
DNTF	76	100
M _{DNTF} :M _{GAP} = 95:5	48	52

3.3. Binding Energy Calculation

Based on the final equilibrium structure of the NVT ensemble, Molecular dynamics simulation is used to calculate the binding energy of the energetic binder GAP and DNTF different crystal surfaces (E_{binding}), which is usually used to characterize the strength of the interaction between the components of the composite system, the calculation formula as (1) formula [16]:

$$E_{\text{binding}} = -E_{\text{inter}} = -(E_{\text{total}} - E_{\text{DNTF}} - E_{\text{GAP}}) \quad (1)$$

E_{inter} is the interaction energy between the two components; E_{total} is the total energy of the composite system; E_{DNTF} is the single-point energy of the DNTF crystalline surface after removing the polymer molecular chain; and E_{GAP} is the single-point energy of the polymer after removing the DNTF crystalline surface, all in Kcal/mol. The binding energies of the polymer and the different crystal surfaces of DNTF were obtained separately according to (1). The results are listed in Table 3.

Table 3. Binding energy between GAP and DNTF (0 1 1) and DNTF (1 0 1) interfaces.

Composite System	Calculation Parameters	E_{total} (kcal·mol ⁻¹)	$E_{\text{explosive}}$ (kcal·mol ⁻¹)	E_{binder} (kcal·mol ⁻¹)	E_{binding} (kcal·mol ⁻¹)
GAP/DNTF (0 1 1)	Energy	-48,551.8	-48,753.5	508.9	307.2
	vdW	-5626.3	-5552.3	23.7	97.7
	Electrostatic interaction	-8781.2	-9357.9	620.4	43.7
GAP/DNTF (1 0 1)	Energy	-47,617.5	-48,117.2	237.7	262.5
	vdW	-5369.2	-5392.3	-65.0	88.1
	Electrostatic interaction	-8117.6	-8738.1	584.8	35.7

The higher the binding energy, the stronger the interaction between the components and the more stable the system will be. Therefore, the binding energy calculation has an important influence on the compatibility of DNTF with GAP and the thermal stability of the energy-containing system. It also significantly reduces the frictional heat generation energy between DNTF and the contact surface and decreases the probability of frictional ignition. As shown in Table 3, the non-bonding energy of the bonding energy contains both vdW (van der Waals force) and electrostatic interaction, and the electrostatic interaction energy in the GAP/DNTF (0 1 1) interface system is 97.7 kJ/mol, which contributes 31.8% to the bonding energy. The electrostatic interaction energy in the GAP/DNTF (1 0 1) interface system is 199.59 kJ/mol, which contributes 33.5% to the binding energy, indicating that the interaction between GAP molecules and DNTF crystals is dominated by electrostatic forces. The binding energies of both GAP/DNTF (0 1 1) and (1 0 1) interface systems were positive, indicating that the interfaces between the binder and the explosive were both able to exist stably; the binding energy of the GAP/DNTF (0 1 1) interface system was 307.2 kcal/mol higher than that of GAP/DNTF (1 0 1), 262.5 kJ/mol, by 44.7%, indicating that the interaction strength of GAP/DNTF (0 1 1) was significantly higher than that of GAP/DNTF (1 0 1). GAP/DNTF (0 1 1) was significantly higher than that of GAP/DNTF (1 0 1), indicating that GAP was more compatible with DNTF (0 1 1) and bound more strongly. The results of the bond energy calculation for GAP/DNTF show that the higher the bond energy between the DNTF interface and the polymer GAP, the stronger they are bonded and the lower the interfacial slip, so that the probability of frictional ignition will be significantly lower. The results of the binding energy calculation of this system are in good agreement with the trend of the test results of the friction sensitivity of the GAP/DNTF

cladding down to 52%, which better reflects the intrinsic factor of the influence of GAP as a cladding layer on the friction sensitivity of DNTF. In addition, it is mentioned in the literature [17] that Gibbs free energy also exists at the interface of solid and liquid. The smaller the value of the Gibbs free energy, the better the thermal stability and toughness of the system, and the less it is affected by temperature. It can be inferred that the less likely it is to generate hot spots stimulated by external unexpected energy, which is might be profit to reduce the sensibility of the GAP/DNTF system.

3.4. Mechanical Properties Calculation

The main parameters of the elastic mechanical properties include the elastic coefficient, the effective isotropic modulus, and Poisson's ratio.

The stress-strain (σ - ε) relationship for the stressed system obeys generalized Hooke's law [18,19].

$$\sigma_i = C_{ij}\varepsilon_j \quad (2)$$

The σ_i is the stress tensor, GPa; the ε_j is the strain tensor, %; C_{ij} ($i, j = 1-6$) is the symmetric matrix of elasticity coefficients, characterizing the stress-strain relationship; the larger the value, the greater the stress required to produce the same strain.

Theoretically, for describing the stress-strain behavior of an arbitrary material, 21 independent variables are required since $C_{ij} = C_{ji}$. This can be simplified by using the Lamé coefficients, as shown in Equation (3) [20,21].

$$[C_{ij}] = \begin{bmatrix} \lambda + 2\mu & \lambda & \lambda & 0 & 0 & 0 \\ \lambda & \lambda + 2\mu & \lambda & 0 & 0 & 0 \\ \lambda & \lambda & \lambda + 2\mu & 0 & 0 & 0 \\ 0 & 0 & 0 & \mu & 0 & 0 \\ 0 & 0 & 0 & 0 & \mu & 0 \\ 0 & 0 & 0 & 0 & 0 & \mu \end{bmatrix} \quad (3)$$

Static mechanical property analysis of the NVT-ensemble MD simulation data at equilibrium was performed to obtain the elastic coefficients (C_{ij}) and effective isotropic moduli, including the Young modulus (E), shear modulus (G) and bulk modulus (K), as well as K/G values and Cauchy pressure (C_{12} - C_{44}) for different crystalline interface models of GAP and DNTF. Based on the Lamé coefficients and the phase relationship between isotropic material moduli [21-23]:

$$E = \frac{\mu(3\lambda + 2\mu)}{\lambda + \mu} \quad (4)$$

$$K = \lambda + \frac{2}{3}\mu \quad (5)$$

$$G = \mu \quad (6)$$

$$\nu = \frac{\lambda}{2(\lambda + \mu)} \quad (7)$$

The Poisson's ratio (ν) of the composite system can be obtained according to Equation (8), and the results of each modulus calculation are shown in Table 4.

$$E = 2G(1 + \nu) = 3K(1 - 2\nu) \quad (8)$$

The modulus parameter of the mechanical properties can be used as an indicator to evaluate the stiffness of the material but also as a measure of the material's ability to resist elastic deformation, and the plastic and fracture properties of the material are associated with the modulus. The coefficient of elasticity C reflects the different elastic effects of the material at each location. Young modulus, bulk modulus, and shear modulus can all be used to measure the strength of the material's stiffness, i.e., its ability to resist elastic

deformation of the material under the action of external forces [24]. The shear modulus (G) is related to the stiffness, which indicates the ability to prevent plastic deformation of the material, and the larger its value, the higher the stiffness and yield strength of the material; the bulk modulus (K) can also be used to correlate the fracture strength of the material, and the larger its value, the greater the energy required to fracture the material, i.e., the greater the fracture strength of the material.

Table 4. Mechanical properties of different GAP and DNTF crystal surfaces.

Modules/GPa	GAP/DNTF (011)	GAP/DNTF (101)	DNTF
C_{11}	2.9624	2.0087	12.8557
C_{22}	7.2005	8.5956	10.6884
C_{33}	7.8268	8.4528	9.1765
C_{44}	2.8645	3.1927	2.1781
C_{55}	1.8319	1.8894	2.0604
C_{66}	1.0651	2.2839	8.0035
C_{12}	2.9988	3.3890	3.2970
C_{13}	1.8833	3.4845	1.1050
C_{23}	3.9747	5.5195	3.2776
E	4.8566	5.8189	10.4586
γ	0.1850	0.2644	0.1531
K	3.0786	3.4359	5.0247
G	1.9205	2.4553	4.5350
K/G	1.2539	1.7891	1.1080
ν	0.2644	0.3282	0.1531
$C_{12}-C_{44}$	0.1343	0.1963	1.1189

The ratio of bulk modulus to shear modulus (K/G) is used to measure the toughness of a material system, i.e., the ability of a material to withstand large deformations under impact or vibration loads without being damaged. K/G is also used to measure the ductility of a material, and the larger the value, the better the ductility of the material [24]. Like K/G , the Cauchy pressure ($C_{12}-C_{44}$) can also predict the ductility of the system, i.e., the ability of the material to deform without cracking; it is also used to reflect the degree of brittleness of the material; with negative values of the Cauchy pressure, the material is brittle, and the smaller the negative value, the more brittle it is. Conversely, when the Cauchy pressure is positive, it indicates that the material is more ductile and shows toughness. Poisson's ratio (ν) is defined as an elastic constant for the ratio of the transverse deformation to the longitudinal deformation when the material is deformed by tensile or compressive forces. The data on the mechanical property parameters of the energetic binder GAP/DNTF for different crystalline interface systems and pure DNTF are shown in Table 4.

With reference to the parameters of the DNTF crystals, it is easily seen that the energetic binder GAP effectively enhances the isotropic material modulus of the DNTF crystals. Compared to the pure DNTF crystals, the Young modulus (E), bulk modulus (K), and shear modulus (G) of the GAP/DNTF (0 1 1) and (1 0 1) composite systems decreased, indicating that the hardness, yield strength, and fracture strength of DNTF decreased, its stiffness decreased, its elasto-plasticity increased, and Poisson's ratio increased [21]. The K/G , and values of the GAP/DNTF (0 1 1) facet system and the GAP/DNTF (1 0 1) facet system are higher than those of pure DNTF crystals, and both systems have positive $C_{12}-C_{44}$ values. It can be concluded that the energetic binder GAP can improve DNTF ductility while also improving toughness. According to the above analysis and the aforementioned impact sensitivity test data, it can be seen that GAP as a cladding layer of DNTF can effectively improve the mechanical properties of DNTF, especially the elasto-plasticity enhancement of the system, which can better absorb the impact energy of external stimuli and reduce the probability of impact ignition of DNTF explosives.

It is thus shown that the reduction of impact sensitivity of GAP/DNTF cladding from 76% to 48% is mainly due to the fact that GAP as a cladding layer greatly improves

the elasto-plastic mechanical properties of DNTF, so the results of molecular dynamics calculations of the mechanical properties of the GAP/DNTF system better reflect the essential reasons for the significant reduction of impact sensitivity of GAP/DNTF cladding on a macroscopic scale.

The E, K, G, and C_{12} - C_{44} values of the GAP/DNTF (1 0 1) interfacial crystals are higher than those of the GAP/DNTF (0 1 1) system. The mechanical modulus of the DNTF (0 1 1) surface, as the first growth surface of the crystal, is smaller than that of the interfacial system corresponding to the DNTF (1 0 1) surface, which will help to improve the mechanical properties of [21].

4. Conclusions

(1) The SEM microscopic morphological characterization shows that the surface of pure DNTF is smooth and flat, and the surface roughness of DNTF increases after GAP coating. A white gelatinous layer is observed on the surface of the original DNTF grains after magnification, indicating that GAP has a better coating effect on DNTF crystals.

(2) The mechanical sensitivity test shows that using GAP as the cladding layer of DNTF crystal can significantly reduce the sensitivity. DNTF sensitivity, impact sensitivity reduced from 76% to 48%, and friction sensitivity reduced from 100% to 52% will help improve the safety of explosives. At the same time, the mechanical sensitivity test results also show that the coating effect of GAP on DNTF is good.

(3) The binding energy of the GAP/DNTF (0 1 1) interfacial system (307.2 kcal/mol) was higher than that of the GAP/DNTF (1 0 1) system (262.5 kcal/mol), indicating that GAP was more compatible with DNTF (0 1 1) and had a stronger and more stable binding. The high binding energy of the GAP/DNTF interfacial system is one of the main intrinsic reasons for its significantly lower friction sensitivity.

(4) Molecular dynamics calculations show that the polymer GAP effectively enhances the isotropic material modulus of DNTF crystals, resulting in less rigidity, more flexibility, and better ductility and toughness of DNTF, which helps the system absorb external impact energy and reduce the impact susceptibility of the GAP/DNTF system.

In summary, GAP can be referred to as a better cladding layer for DNTF, which is feasible for inhibiting the problem of DNTF crystallization in propellants. This study provides a potential new crystallization inhibition pathway for the DNTF modified double-base propellants. Nevertheless, this study still has some limitations. For example, consider whether the propellant calendaring process at high temperature affects the crystal structure of the cladding, as well as a more comprehensive characterization of the thermal properties of the GAP-coated DNTF. Next, we will also continue to study this in depth.

Author Contributions: Conceptualization, J.Y.; methodology, J.Y.; validation, Y.Q., H.S., Y.L. and H.Z.; formal analysis, Y.Q., H.S. and H.Z.; data curation, Y.Q. and Y.L.; writing—original draft preparation, Y.Q.; writing—review and editing, J.Y.; visualization, R.W., J.C. and X.L. All authors have read and agreed to the published version of the manuscript.

Funding: This study was carried out within the project “Research on the mechanism of DNTF crystallization in propellant and inhibition technology”, projects No.20210579 is funded by the Bottleneck Technology and JCQJ Foundation.

Data Availability Statement: The data presented in this study are openly available.

Conflicts of Interest: The authors declare no conflict of interest.

References

1. Zheng, W.; Wang, J.; Ren, X.; Zhang, L.; Zhou, Y. An Investigation on Thermal Decomposition of DNTF-CMDB Propellants. *Propellants Explos. Pyrotech.* **2010**, *32*, 520–524. [[CrossRef](#)]
2. Zheng, W.; Wang, J.N.; Han, F.; Tian, J.; Song, X.D.; Zhou, Y.S. Chemical Stability of CMDB Propellants Containing DNTF. *Chin. J. Explos. Propellants* **2010**, *33*, 10–13.
3. Tian, J.; Wang, B.C.; Sang, J.F.; Zhang, F.P.; Wang, J.N. Experimental research on the properties of CMDB propellant containing DNTF. *Chin. J. Explos. Propellants* **2015**, *38*, 76–79.

4. Pang, J.; Wang, J.N.; Zhang, R.E.; Xie, B. Application of CL-20, DNTF and FOX-12 in CMDB propellants. *Chin. J. Explos. Propellants* **2005**, *28*, 19–21.
5. Li, X.T. Crystallization of RDX from a composite modified double-base propellant. *Acta Armamentarii* **1979**, *1*, 23–27.
6. Jia, Z.N.; Yi, L.H. Research on a surface coating method to prevent crystallization of RDX. *Chin. J. Explos. Propellants* **1994**, *16*, 6–8.
7. Jia, Z.N. Research on the crystallization phenomenon and anti-crystallization of RDX. *Acta Armamentarii* **1995**, *16*, 37–40.
8. Zheng, W.; Xie, B.; Hu, Q.; Cao, L.; Wang, J.N.; Zhang, J. Crystal analysis of DNTF-containing modified double-based propellants. *J. Solid Rocket Technol.* **2016**, *39*, 509–512.
9. Liang, L.; Yun, N.; Geng, X.H.; Lin, S.T. Synthesis and properties of (glycidyl azide polymer) GAP. *J. North Univ. China (Soc. Sci. Ed.)* **2014**, *35*, 177–181.
10. Badgujar, D.M.; Talawar, M.B.; Zarko, V.E.; Mahulikar, P.P. New directions in the area of modern energetic polymers: An overview. *Combust. Explos. Shock Waves* **2017**, *53*, 371–387. [[CrossRef](#)]
11. Xia, L.; Xiao, J.J.; Fan, J.F.; Zhu, W.; Xiao, H.M. Molecular dynamics simulation of the mechanical properties and interfacial interactions of nitrate plasticizers. *Acta Chim. Sin.* **2008**, *66*, 874–878.
12. Wang, H.; Gao, J.; Tao, J.; Luo, Y.M.; Jiang, Q.L. Safety and molecular dynamics simulations of DNTF/HATO hybrid systems. *Chin. J. Energ. Mater.* **2019**, *27*, 897–901.
13. Meng, L.L.; Qi, X.F.; Wang, J.N.; Fan, X.Z. Molecular dynamics simulation and experimental study of the plasticization properties of NC by DNTF. *Chin. J. Explos. Propellants* **2015**, *38*, 86–89.
14. Liu, C.; Zhao, Y.; Xie, W.X.; Liu, Y.F.; Huang, H.T.; Zhang, W.; Zhang, X.H. Molecular dynamics simulation of interfacial interactions in GAP/Al composite systems. *New Chem. Mater.* **2018**, *46*, 186–189.
15. Li, Z.F.; Feng, Z.G.; Hou, Z.L. Synthesis and performance analysis of azide binder GAP. *J. Qingdao Inst. Chem. Technol.* **1997**, *18*, 155–163.
16. Xiao, J.J.; Wang, W.R.; Chen, J.; Ji, G.F.; Zhu, W.; Xiao, H.M. Study on structure, sensitivity and mechanical properties of HMX and HMX-based PBXs with molecular dynamics simulation. *Comput. Chem.* **2012**, *999*, 21–27. [[CrossRef](#)]
17. Eslami, H.; Khanjari, N.; Müller-Plathe, F. A local order parameter-based method for simulation of free energy barriers in crystal nucleation. *J. Chem. Theory Comput.* **2017**, *13*, 1307–1316. [[CrossRef](#)]
18. Ma, S.; Li, Y.J.; Li, Y.; Luo, Y.J. Research on structures, mechanical properties, and mechanical responses of TKX-50 and TKX-50 based PBX with molecular dynamics. *J. Mol. Model* **2016**, *22*, 1–11. [[CrossRef](#)]
19. Weiner, J.H. Statistical Mechanics of Elasticity. *J. Appl. Mech.* **1984**, *51*, 707–708. [[CrossRef](#)]
20. Xiao, J.J.; Huang, Y.C.; Hu, Y.J.; Xiao, H.M. Molecular dynamics simulation of mechanical properties of TATB/fluorine-polymer PBXs along different surfaces. *Sci. China Ser. B Chem.* **2005**, *48*, 504–510. [[CrossRef](#)]
21. Wang, K.; Li, H.; Li, J.Q.; Xu, H.X.; Zhang, C.; Lu, Y.Y.; Fan, X.Z.; Pang, W.Q. Molecular dynamic simulation of performance of modified BAMO/AMMO copolymers and their effects on mechanical properties of energetic materials. *Sci. Rep.* **2020**, *10*, 1–17. [[CrossRef](#)] [[PubMed](#)]
22. Xin, D.R.; Han, Q. Study on thermomechanical properties of cross-linked epoxy resin. *Mol. Simulat.* **2015**, *41*, 1081–1085. [[CrossRef](#)]
23. Hu, Y.Y.; Chen, C.Y.; Chen, K. Molecular Dynamics Simulation of Mechanical Properties of Single-base and Double-base Propellants. *J. Nanjing Xiaozhuang Univ.* **2007**, *23*, 47–50.
24. Xing, X.W.; Yuan, J.M.; Li, Y.; Sha, H.B.; Luo, Y.M.; Jiang, Q.L. Molecular dynamics calculation of the effect of GAP-ETPE on the performance of DNTF explosives. *J. Ordnance Equip. Eng.* **2022**, *43*, 293–298.

Disclaimer/Publisher’s Note: The statements, opinions and data contained in all publications are solely those of the individual author(s) and contributor(s) and not of MDPI and/or the editor(s). MDPI and/or the editor(s) disclaim responsibility for any injury to people or property resulting from any ideas, methods, instructions or products referred to in the content.